

See discussions, stats, and author profiles for this publication at: <https://www.researchgate.net/publication/5819255>

Role of the Intracellular Cavity in Potassium Channel Conductivity

ARTICLE *in* THE JOURNAL OF PHYSICAL CHEMISTRY B · JANUARY 2008

Impact Factor: 3.3 · DOI: 10.1021/jp0747813 · Source: PubMed

CITATIONS

8

READS

16

3 AUTHORS, INCLUDING:



Simone Furini

Università degli Studi di Siena

44 PUBLICATIONS 388 CITATIONS

SEE PROFILE

Role of the Intracellular Cavity in Potassium Channel Conductivity

Simone Furini,^{*,†} Francesco Zerbetto,[‡] and Silvio Cavalcanti[†]

Department of Electronics, Computer Science and Systems, University of Bologna, Viale Risorgimento, 2 I-40136, Bologna, Italy, and Department of Chemistry "G. Ciamician", University of Bologna, Via F. Selmi, 2 I-40126, Bologna, Italy

Received: June 20, 2007; In Final Form: September 24, 2007

The role of several fragments of the potassium channel KcsA has been examined by the Poisson–Nernst–Planck (PNP) theory. The efficiency of the computational method allowed comparing a large number of channel models, with different intracellular gate openings, partial atomic charges, and amino acid sequences. Perhaps counter-intuitively, the calculated ion current decreases when the mean radius of the entrance cavity increases. Widening of the vestibule, in fact, increases the volume accessible to water, which is the volume with a high dielectric constant. In turn, water screens the attractive charges of the P-loop backbone. The backbone charges of the M2 helices instead oppose the entrance of potassium ions through a complicated mechanism that can be separated in the activity of two interfering dipoles. The conductance of the KcsA models increased when two neutral residues in M2 were mutated to glutamic acid, in agreement with experimental results (Brelidze, T. I.; Niu, X.; Magleby, K. L. *PNAS* 2003, 100, 9017–9022). As a general conclusion, a relation between channel conductance and potassium concentration in the intracellular cavity emerged. Although the ion transport is the result of the fine balance of a number of different effects, the experimental results can be reproduced quantitatively only on the basis of electrostatic forces, which are the only driving forces modeled by the PNP theory.

Introduction

Potassium channels regulate the flux of K^+ ions through cell membranes and take part in several physiological functions such as cell excitability and secretion.¹ When dysfunctional, ion channels give rise to a number of diseases,² which renders the establishing of the molecular determinants of channel function of profound interest, both for the biological and for the medical sciences. In this study, the relation between atomic structure and conductance in potassium channels is theoretically analyzed, by a continuum model of electrodiffusion in the Poisson–Nernst–Planck (PNP) formulation.

The atomistic comprehension of the role of the protein architecture on channel conductance can be reached by computer simulations, which require the detailed knowledge of the structure of the protein. The crystallographic structures of five distinct potassium channels (KcsA, MthK, KvAP, KirBac1.1, and Kv1.2) reveal a common architecture of the pore.^{3–7} Four alpha subunits are symmetrically arranged around the channel axis. Each subunit has at least two transmembrane helices (M1 and M2) separated by a re-entrant P-loop and by the selectivity filter (Figure 1). In spite of the high similarity of their architectures, the conductance of potassium channels varies widely.¹ Channels belonging to the BK family have a conductance almost 2 orders of magnitude higher (~ 200 pS) than other potassium channels, such as the voltage gated channels.⁸ The selectivity filter itself is not likely to cause this variability, since it retains the same atomic structure in channels characterized by very different conductances. Conversely, the cytoplasmatic, water-filled vestibule at the center of the membrane shows some

variability.⁹ This intracellular cavity regulates the exchange of ions between the intracellular compartment and the selectivity filter; it contributes to the channel selectivity¹⁰ and must play an essential role in channel conductance. Perhaps surprisingly, the theoretical demonstration of the role of the structure of the cavity in determining the conductivity is still lacking.

The intracellular cavity differs in the structures available to date. The cavity is almost closed in the crystallographic structure of the KcsA channel because of the presence of a bundle between the M2 helices. Indeed, KcsA was likely crystallized in the closed state, and the M2 helices were identified as the intracellular gate.⁴ On the contrary, KvAP and MthK were crystallized in the open state.^{5,6} Both of the crystallographic structures of KvAP and MthK show a wider intracellular opening than KcsA owing to a movement of the M2 helices.^{11,12} The movement is more pronounced in MthK than in KvAP so that the intracellular cavity of the former is wider.

The influence of the intracellular gate opening on the electrostatic potential inside the cavity has been studied in KcsA by Poisson–Boltzmann theory.¹³ A lumen similar to that of the experimental structure of KvAP was found optimal for conductance since it provides a flat energy profile for the ion transport from the bulk solution to inside the cavity. The wider opening revealed in MthK hardly improves the probability of entrance inside the cavity of potassium. However, experimental data suggest a wider pore in the BK potassium channels, and a relation between the wider pore and the higher conductance was suggested.¹⁴

Additionally, to the amount of gate opening, the behavior of ions in the cavity is affected by the charge distribution in the protein. Charges from the backbone and the sidechains may hinder or accelerate ion passage. Poisson–Boltzmann calculations revealed the important role of the backbone charges in

* Corresponding author. Phone: +390512093067. Fax: +390512093540. E-mail: sfurini@deis.unibo.it.

[†] Department of Electronics, Computer Science and Systems.

[‡] Department of Chemistry "G. Ciamician".

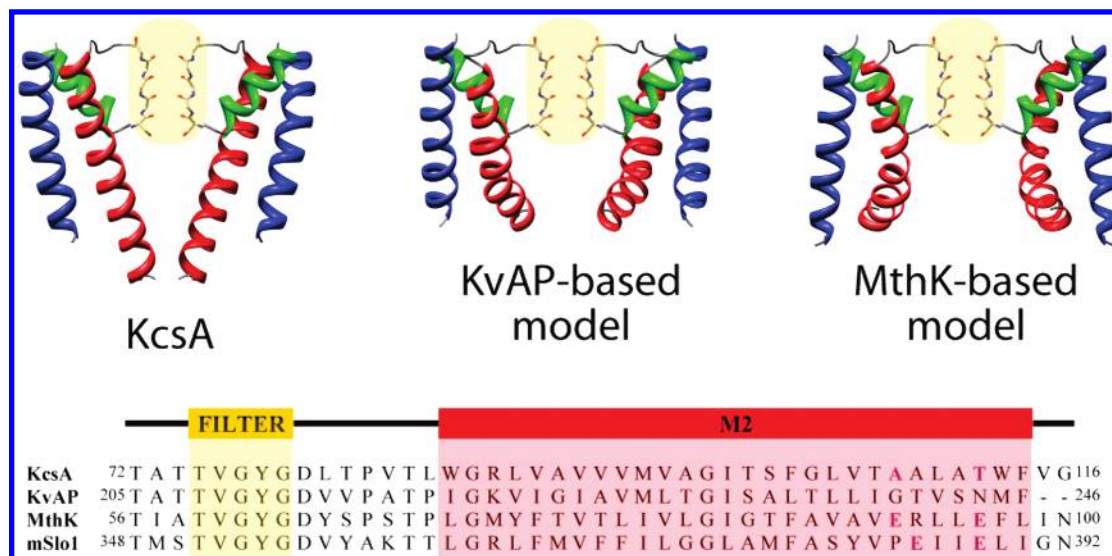


Figure 1. Channel models and amino acid sequences. The crystallographic structure of KcsA is shown, together with the structures of the KvAP- and MthK-based models. For the sake of clarity, only two of the four channel subunits are shown (M1 helices in blue, M2 in red and P-loop in green). The amino acid sequences of KcsA, KvAP, MthK, and mSlo1 (BK potassium channel) are shown at the bottom. The amino acids A108 and T112 in the KcsA sequence are highlighted in purple, as the negatively charged residues in the M2 helix of MthK and mSlo1.

the P-loop alpha helices.¹⁵ In practice, the local atomic charges of the P-loop helix generate an electric dipole, which points toward the cavity and attracts potassium ions. Indeed, a potassium ion inside the cavity was experimentally revealed in the crystallographic structure of KcsA.⁴ The P-loop backbone charges must therefore be important for the conduction mechanism, but to the best of our knowledge, this effect has not been quantified yet.

The role of the side chain charges on the channel functioning has been experimentally investigated in several channel families.^{16–21} Concerning potassium channels, it was found that negatively charged residues in the M2 helices, which are highly conserved in BK potassium channels, are crucial for the high conductance phenotype.^{22,23} An increase in the potassium concentration inside the cavity was proposed as the mechanism by which negatively charged residues in M2 increase the conductance.²³

In this computational study, we demonstrate that KcsA conductivity is highly sensitive to the presence of negative residues and that, for physiological concentrations of potassium, they cause an increase of its concentration inside the cavity. The potassium concentration inside the cavity emerges as a general driving force that regulates channel conductance. Electrostatic interactions lie at the core of this mechanism.

Methods

Channel Models. A model of KcsA in the closed state was defined according to its high-resolution crystallographic structure (Protein Data Bank, pdb 1K4C²⁴). The model includes the pore region of the channel, from amino acid 28 to 114. Acetyl and *N*-methyl groups were added to the N and C terminals. Hydrogen atoms were added by Amber8.²⁵ All of the amino acids were taken in the default protonation state, except for glutamate 71, which was assumed protonated.²⁶

The experimental structures of KvAP (pdb 1LNQ⁶) and MthK (pdb 1ORQ⁵) were used as templates for the KcsA open state. The amino acid sequences of KcsA, KvAP, and MthK were aligned using the T-Coffee software (Figure 1).²⁷ Two models of KcsA in the open state were defined, moving the KcsA backbone atoms to the analogous atoms of KvAP and MthK. The crystallographic structures of KcsA, KvAP, and MthK differ

mainly in the M2 helices, with minor differences located in the M1 helices. Therefore, only the KcsA amino acids from 28 to 51 and from 87 to 114 were displaced to open the channel. The resulting models have the backbone structure of KvAP and MthK, while the sidechains orientation of KcsA is preserved. In addition to the KvAP and MthK based models, a series of “in-between” models were defined, gradually shifting the channel structures one into another.

The KcsA models were used to analyze the role of the gate opening, without taking into account the possible biasing contribution of the amino acid sequence. Since potassium ions enter the cavity in the hydrated form,⁴ only channel models with an intracellular gate wider than a hydrated potassium ion (3.31 Å, corresponding to the first hydration shell²⁸) were considered. The narrowest channel model used here is referred to as the KcsA-based model. The names KvAP-based model and MthK-based model are adopted for the KcsA open structures modeled on KvAP and MthK (Figure 1).

To study the influence of the side chain charges on the channel conductance, the models of three mutated channels were defined (A108E, T112E, and A108E/T112E). The sidechains of the mutated amino acids were manually placed in the best rotamer state by the software DeepView.²⁹

Numerical Solver. PNP theory describes the steady-state distribution of a continuous system of mobile charges, in the presence of concentration gradients and electric fields. When PNP theory is applied to membrane channels, the mobile charges are the ionic species in solution, whose distributions are described by the concentrations $C_i(\vec{r})$ (where i is the i th ion and \vec{r} its the position in space). Concentration gradients and electric fields cause a flux of ions (J_i) modeled by the drift-diffusion equation (Nernst–Planck equation):

$$J_i(\vec{r}) = -D_i(\vec{r}) \left\{ \nabla C_i(\vec{r}) + \frac{e}{k_B T} z_i C_i(\vec{r}) \nabla \phi(\vec{r}) \right\} \quad (1)$$

where, ϕ is the electric potential; D_i and z_i are the diffusion coefficient and the charge of the i th ion; e is the elementary charge; k_B is the Boltzmann constant; and T is the temperature. Ion concentrations and electric potential can be computed by solving the Poisson (eq 2) and the continuity equations (eq 3):

$$\nabla \cdot \{\epsilon(\vec{r}) \nabla \phi(\vec{r})\} = -\rho(\vec{r}) - \sum_{i=1}^N e z_i C_i(\vec{r}) \quad (2)$$

$$\nabla \cdot \mathbf{J}_i(\vec{r}) = 0 \quad (3)$$

In the Poisson equation, ϵ is the dielectric constant and ρ is the fixed charge distribution of the protein and the lipid bilayer atoms. In this study, only the protein charge distribution was explicitly modeled, while the lipid bilayer was supposed electrically neutral. Two monovalent ion species were included in the mathematical model, to simulate respectively potassium and chloride ions.

The PNP differential equation set, eqs 2 and 3, was solved numerically.³⁰ To improve the accuracy of the discretization procedure, a cylindrical grid was implemented. In a cylindrical grid, the volume is divided in slices orthogonal to the cylinder axis, and each slice is divided in segments and rings. As a consequence, the grid elements are tinier close to the cylinder axis and larger far from the axis. The grid axis was chosen as the channel axis to provide a more accurate discretization in this region, where the analysis is focused.

The grid axis length was set to twice the channel length, and the grid radius was set to 1.5 times the channel external radius. The number of grid points was 140 along the axis (distance 0.05 nm), 150 along the radial direction (distance 0.025 nm), and 72 along the angular direction (distance 0.087 rad). The iterative procedure used to solve eqs 2 and 3 was stopped once the distance between consecutive solutions fell below 10^{-10} mV for electric potential and 10^{-10} mM for ion concentrations.

The relative dielectric constant was set to 2 in protein and 80 in water. A volume with low dielectric constant ($\epsilon = 2$) was introduced around the channel, to mimic the presence of the lipid bilayer. The aromatic residues tyrosine 45 and tryptophan 113 were used to define the upper and lower boundary of the lipid bilayer. Diffusion coefficients were set to the experimental bulk values in water outside the channel ($D_{K^+} = 1.96 \times 10^{-9}$ m²/s and $D_{Cl^-} = 2.03 \times 10^{-9}$ m²/s³¹) and were reduced to 10% inside the channel. A reduction of diffusion coefficients to 10% was sufficient to fit the experimental currents and in line with molecular dynamics simulations of narrow ion channels.^{32,33} The radii and partial atomic charges of the protein atoms were set to the values proposed by Nina et al.³⁴ The effect of their variation has been reported before.³⁰

Results

Intracellular Gate Opening. Perhaps counter-intuitively, when the mean radius of the intracellular cavity increases from 0.36 nm to 0.63 nm, the calculated conductance decreases by ~20%, regardless of the applied membrane potential (Figure 2). A mean radius of 0.63 nm corresponds to the KvAP-based model. Further increase of the gate opening does not affect the channel conductance. The currents through the KvAP- and the MthK-based models differ less than 1%, in spite of an increase in the mean internal radius of ~30%. The conductance values for gate openings from the KvAP- to the MthK-based model are in good agreement with experimental data (77.3 ± 0.8 pS versus 75.6 ± 10 pS, with membrane potential set to 100 mV and ion concentrations set to 100 mM; 96.0 ± 1.0 pA versus 95.6 ± 11 pA, with membrane potential set to 25 mV and ion concentrations set to 100 mM³⁵).

The gate opening affects the electric potential and the potassium concentration only inside the intracellular cavity (Figure 3). Electric potential and concentration are almost

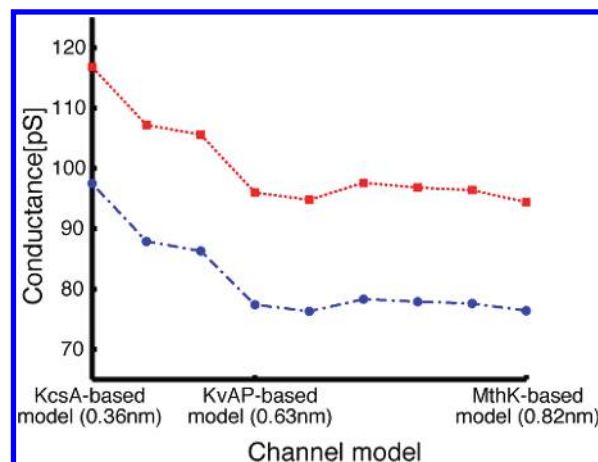


Figure 2. Channel conductance at different gate openings. The blue dashed line (circular points) and the red dotted line (square points) show the channel conductance when the membrane potential is set to 100 mV and 25 mV, respectively. The x axis ranges from the KcsA-based model to the MthK-based model. Ticks on the x axis highlight the location of the KcsA-, KvAP- and MthK-based model. The mean radius of cavity in these structures is shown. Potassium and chloride concentrations are set to 100 mM.

unchanged in the selectivity filter, in agreement with previous results by Monte Carlo free energy integration.³⁶ The potential in the intracellular cavity is more positive in wider channels, and consistently, the potassium concentration is lower. Potassium concentration exhibits a peak below the selectivity filter (intracellular side). This peak is preserved in all of the channel models, regardless of the opening extent (Figure 3). The position of this peak resembles the position of the potassium ion experimentally revealed in the KcsA crystallographic structure.⁴ The peak value decreases from 700 mM in the KcsA-based model to 420 mM in the KvAP-based model (membrane potential set to 100 mV; ion concentrations set to 100 mM). Further channel openings cause a minor decrease in the potassium concentration peak.

The decrease in current, caused by the gate opening, is due to the presence of the P-loop backbone charges (see below). These charges stabilize the presence of a potassium ion inside the cavity¹⁵ with a nontrivial mechanism. Widening of the vestibule increases the volume accessible to water, that is, the volume with a high dielectric constant. Increasing the volume with high dielectric constant increases the shielding of the P-loop backbone charges and reduces the attraction exerted by these charges on potassium ions. Indeed, according to Poisson–Boltzmann calculations, the stabilization energy provided by the charges of the P-loop backbone on a potassium ion in the cavity is -27.5 kcal/mol in the closed model of KcsA. This energy decreases to -7.0 kcal/mol in a KcsA structure modeled on the KvAP experimental structure.¹³

The geometry of the intracellular cavity was probed experimentally with sugar molecules, and a wide cavity for the BK channels was suggested.¹⁴ This wider cavity has been associated to the high conductance phenotype of BK channels. Actually, according to our results, the wider cavity does not necessarily imply an increase of conductance.

Protein Charge Neutralization. P-Loop Helices. Neutralization of the partial atomic charges of the P-loop backbone atoms causes a sizable decrease of channel current (Table 1). The decrease is not related to the extent of the gate opening. Indeed, KcsA-, KvAP-, and MthK-based models show almost the same current drop by nearly an order of magnitude. The electric potential inside the cavity turns from negative to positive, and

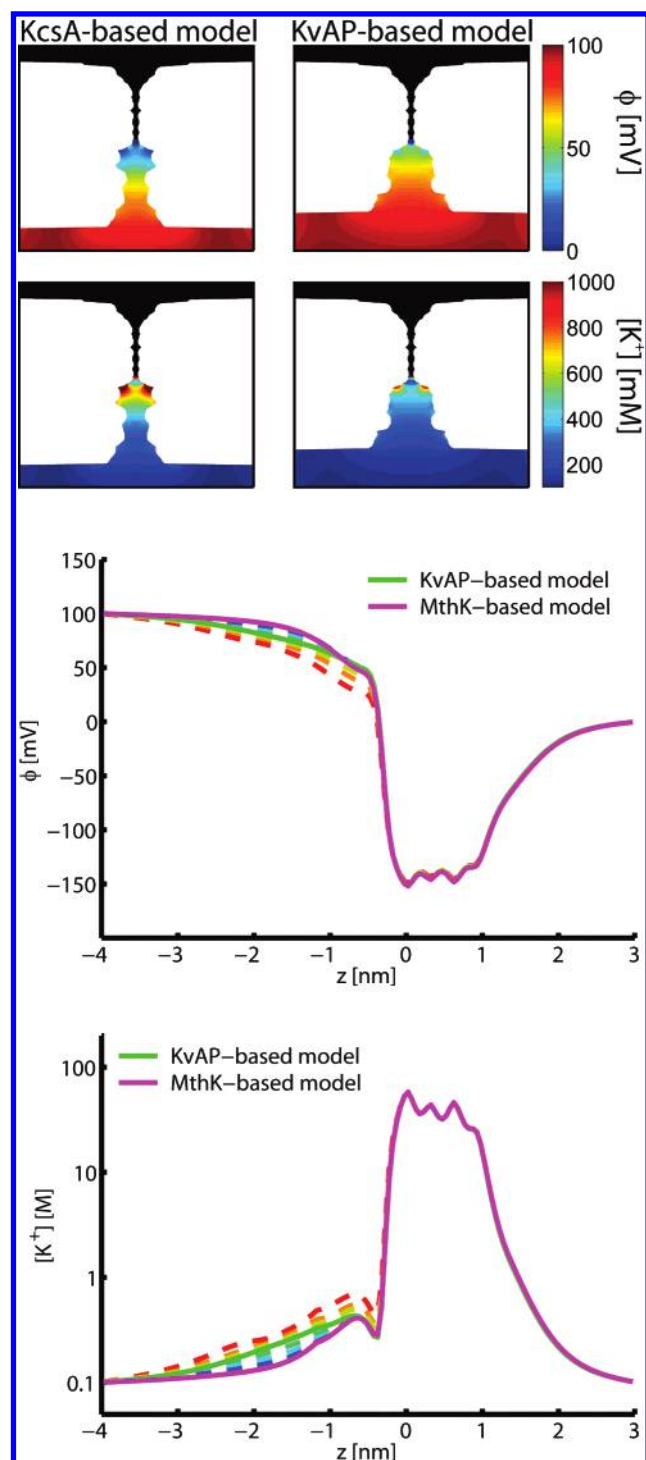


Figure 3. Gate opening: electric potential and K^+ concentration. (Upper panels) Electric potential (ϕ) and potassium concentration ($[K^+]$) inside the KcsA- and the KvAP-based model. The color maps show the electric potential and the potassium concentration on a longitudinal section of the channel. In order to focus the color maps on the intracellular cavity, electric potential and potassium concentrations in the selectivity filter and in the extracellular compartment are not shown. (Bottom plots) Electric potential (ϕ) and potassium concentration ($[K^+]$) along the channel axis. The z axis extends from the intracellular to the extracellular compartment. A logarithmic scale is used for the potassium concentration. Different colors are used for different intracellular gate openings: KcsA-based model in red, color spectrum from red to purple for wider gate openings. Continuous lines are used for the KvAP- and MthK-based model, and dashed lines are used for the other structures. Membrane potential is set to 100 mV, and ion concentrations are set to 100 mM, both for the data in the color maps and for the data in the plots.

the peak in the potassium concentration disappears (Figure 4). Importantly, potential and concentration in the selectivity filter do not change. The applied membrane potential does not affect the decrease in channel current. The percentage variation in the channel current ($\Delta I\%$) almost does not change when the membrane potential ranges from -100 mV to $+100$ mV, as proved by the low standard deviation (Table 2). To further confirm the crucial role of the backbone charges, calculations were repeated removing the side chain charges of the P-loop and retaining the backbone charges. No sizable change in conductance, electric potential, and potassium concentration was observed in these conditions (Table 1; Figure 4).

In a related system, Chatelain et al.³⁷ challenged the role of the electrical dipole generated by the P-loop backbone charges. They showed that the presence of a positive residue close to the P-loop C terminal of a mutated Kir2.1 channel does not change the conductance. This seems to suggest that the P-loop backbone dipole does not play a role in the conduction mechanism. However, comparison of the X-ray structures of KcsA⁴ and KirBac1.1¹⁷ shows that P-loop backbone charges likely play a different role in inward rectifier channels. At odds with the present case, the P-loop helices do not point toward the center of the intracellular cavity, and the sidechains are peripheral with respect to the α helix backbone so that the interplay of the backbone dipole, the atomic charges in the sidechains, and a potassium ion in the cavity could differ.

M1 and M2 Helices. The backbone charges in the M1 helices have no sizable effect on conductance, electric potential, and ion concentrations (Table 1; Figure 4). M1 helices are too far from the chamber to exert a Coulombic effect. On the contrary, a functional role of the M2 backbone charges emerges. Neutralization of the M2 backbone charges causes a sizable increase in the channel current and in the potassium concentration, both for the KvAP- (+17%) and for the MthK-based (+30%) models (Table 1; Figure 4). On the contrary, the neutralization of the M2 backbone charges does not affect the ion transport in the KcsA-based model (Table 1). These results are not affected by the applied membrane potential (Table 2).

In the closed state, M2 helices have a straight axis and effectively generate a single electric dipole. The channel opening is achieved by bending the M2 helices at a hinge glycine (glycine 99 in KcsA). Once the M2 helices are bent, they do not generate a single electric dipole. Each M2 helix is actually split into two helices: one extending from the N-terminal of M2 to the hinge glycine and one extending from the hinge glycine to the C-terminal of M2. As a consequence, the electric dipole of M2 splits into two components: one associated to the N-terminal helix (~ 30 Debye) and one to the C-terminal helix (~ 35 Debye). The negative pole of the dipole associated to the N-terminal helix is close to the channel cavity, while the dipole associated to the C-terminal helix has the positive pole close to the cavity. Consequently, while the former stabilize an ion in the cavity, the latter destabilize it (Figure 4). The interference of the two effects almost balances for structures narrower than the KvAP-based model. When the M2 helices are shifted, as in the crystallographic structure of MthK, the destabilizing dipole dominates. This destabilizing effect counterbalances the decrease of electrical resistance, and consequently the conductance does not vary going from the KvAP- to the MthK-based model. Both the M2 dipoles do not point toward the cavity center, and they are not as important as the P-loop dipole for the channel functioning.

Amino Acid Mutations. The mutation of amino acids alanine 108 or threonine 112 to glutamate increases the channel current

TABLE 1: Computed Channel Currents with a Membrane Potential of 100 mV^a

	KcsA-based model		KvAP-based model		MthK-based model	
	<i>I</i> [pA]	$\Delta I\%$	<i>I</i> [pA]	$\Delta I\%$	<i>I</i> [pA]	$\Delta I\%$
wild-type channel, no neutralized charge	9.75		7.74		7.64	
P-loop backbone	1.11	−89%	1.09	−86%	1.09	−85%
P-loop side chain	9.11	−7%	6.96	−10%	6.96	+9%
M1 backbone	10.28	+5%	8.31	+7%	7.70	+1%
M2 backbone	9.55	−2%	9.04	+17%	9.92	+30%
mutation A108E	12.89	+32%	11.64	+50%	10.24	+34%
mutation T112E	11.71	+20%	11.46	+48%	9.76	+28%
mutations A108E/T112E	14.31	+46%	16.53	+114%	12.87	+68%

^a Ionic currents (*I*) through three channel models are reported, together with data on charge neutralizations and amino acid mutations. The percentage variation in the channel current ($\Delta I\%$) refers to the current in the wild-type channel, same channel model, with no neutralized charge. Potassium and chloride concentrations are set to 100 mM.

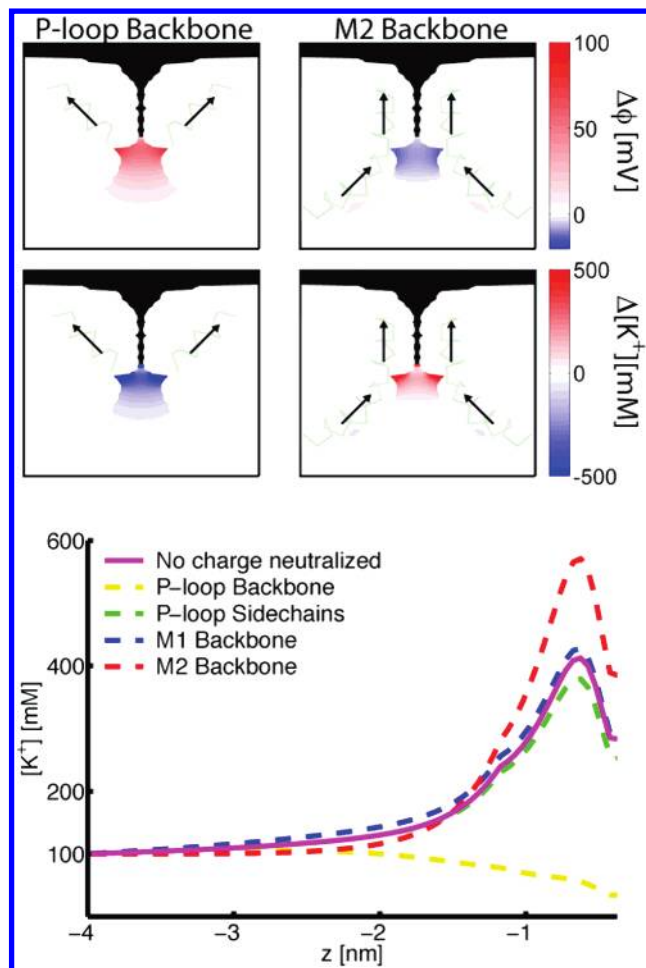


Figure 4. Protein charges neutralization: electric potential and K^+ concentration in the MthK-based model. (Upper panels) Changes in electric potential ($\Delta\phi$) and potassium concentration ($\Delta[K^+]$) induced by the neutralization of the P-loop or M2 backbone charges in the MthK-based model. As in Figure 3, a longitudinal section of the channel is shown and the color maps are focused on the intracellular cavity. P-loop and M2 helices, together with dipole directions (from the negative to the positive pole), are shown. (Bottom plot) Potassium concentration ($[K^+]$) along the channel axis. The *z* axis extends from the intracellular compartment to the bottom of the selectivity filter. Membrane potential is set to 100 mV, and ion concentrations are set to 100 mM, for the data both in the color maps and in the plot.

(Table 1). A rather similar current increase is present in all channel models for the two mutations. Mutating both the residues to glutamate further increases the current (Table 1). The highest increase is observed in the KvAP-based model (+114%), while a smaller increase appears in the KcsA- and

MthK-based models (+46% and +68%). The current increase is not affected by the applied membrane potential (Table 2). Potassium concentration inside the cavity increases in the channel as a consequence of the mutations (Figure 5). The concentration peak below the selectivity filter almost doubles in the channel with the mutations A108/ET112E (Figure 5).

Nimigean et al. measured a considerable increase in the channel current when alanine 108 of KcsA (located facing the cavity) was mutated to aspartate.²² Similarly, Brelidze et al. observed a two-fold decrease of the conductance in the mSlo1 channel, when both glutamate residues of M2 were mutated to asparagines.²³ We found a two-fold increase of current when two negatively charged residues were introduced in M2 (+113% in the KvAP-based model). Brelidze et al. also found experimentally that an increase of the bulk concentration of potassium from 150 mM to 500 mM has the same effect as the presence of two negatively charged residues. In accordance with these experimental data, we revealed the same current in the wild-type channel with potassium bulk concentration set to 500 mM and in the double mutated channel with potassium bulk concentration set to 100 mM.

To analyze the relationship between potassium concentration inside the cavity and conductance, the current through the doubly mutated channel was compared with the current through the wild-type channel at different potassium concentrations (Figure 6). At 20 mM, the current of the mutated channel is more than double the current of the wild-type channel. At 1.6 M, the two channels produce almost the same current. The result agrees with the hypothesis that the conductance increase in the mutated channel is related to the higher potassium concentration inside the cavity. At low bulk concentration, an efficient way to attract potassium ions in the cavity is extremely important to preserve a high conductance value. The negatively charged residues of the mutated channel attract potassium ions in the cavity more efficiently than the wild-type channel. When the bulk concentration is large, the attraction of potassium ions inside the cavity becomes marginal, and the difference between mutated and wild-type channels decreases.

Potassium Concentration in the Cavity as a Conductance Determinant. Analysis of the potassium concentration in the intracellular cavity reveals a relation between the concentration peak and the channel conductance. In Figure 7, the current through the channel is shown as a function of the maximum potassium concentration inside the cavity (measured along the channel axis). Figure 7 includes data from all of the different channel models, atomic charge neutralizations, amino acid mutations, and applied membrane potentials discussed in the previous sections. Data were fitted by a line, in a least-square approach. The cross-correlation index between concentration

TABLE 2: Dependence of the Current Changes on the Membrane Potential^a

	$\Delta I\%$		
	KcsA-based model	KvAP-based model	MthK-based model
P-loop backbone	$(-88.6 \pm 0.2)\%$	$(-85.1 \pm 0.9)\%$	$(-84.8 \pm 0.9)\%$
M2 backbone	$(-3 \pm 1)\%$	$(16.3 \pm 0.8)\%$	$(29.6 \pm 0.5)\%$
mutations A108E/T112E	$(47 \pm 2)\%$	$(113 \pm 1)\%$	$(67.9 \pm 0.9)\%$

^a The percentage variation in the channel current ($\Delta I\%$) refers to the wild-type channel, same channel model, with no neutralized charge. Currents were computed at different membrane potential, ranging from -100 mV to $+100$ mV with a 25 mV step. The mean value of the percentage variation along this range of membrane potential is reported, together with the standard deviation. Potassium and chloride concentrations are set to 100 mM.

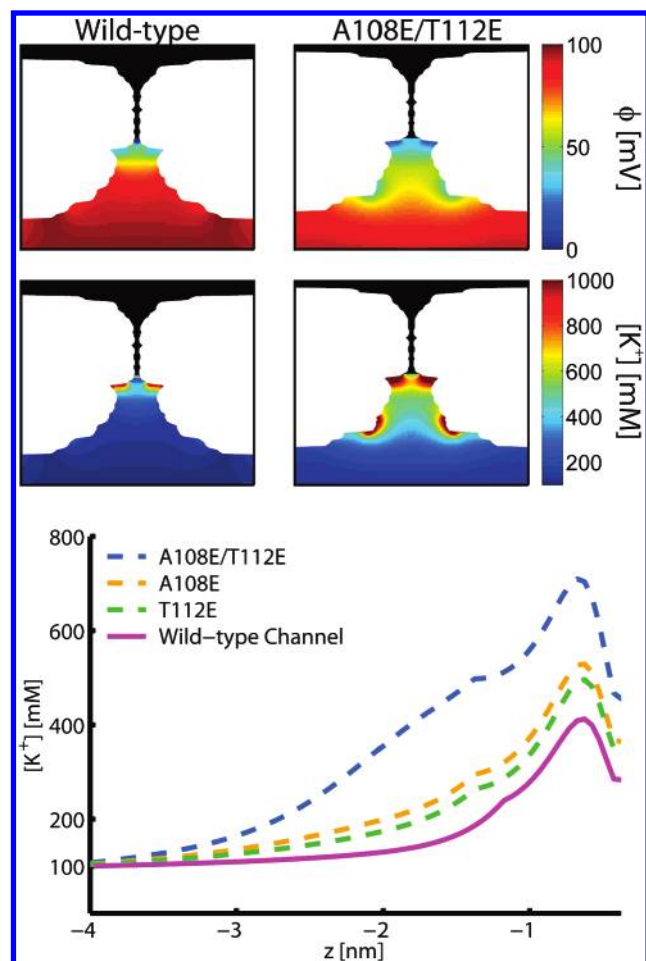


Figure 5. Amino acid mutations: electric potential and K^+ concentration in the MthK-based model. (Upper panels) Electric potential (ϕ) and potassium concentration ($[K^+]$) in the MthK-based model, wild-type or with the A108E/T112E mutations. As in Figure 3, a longitudinal section of the channel is shown, and the color maps are focused on the intracellular cavity. (Bottom plot) Potassium concentration ($[K^+]$) along the channel axis. The z axis extends from the intracellular compartment to the bottom of the selectivity filter. Membrane potential is set to 100 mV, and ion concentrations are set to 100 mM, for the data both in the color maps and in the plot.

and current is 0.96 , and the root-mean-square distance of the computed currents from the interpolating line is 1.2 pA. The sensitivity of the conductance to the potassium concentration inside the cavity is 12.5 pA/M. An important conclusion emerges: there is a strict relationship between channel conductance and potassium concentration in the KcsA cavity.

Discussion

Electrodiffusion (PNP) theory is able to simulate accurately a large number of experimental data in ion channels.³⁸ Once

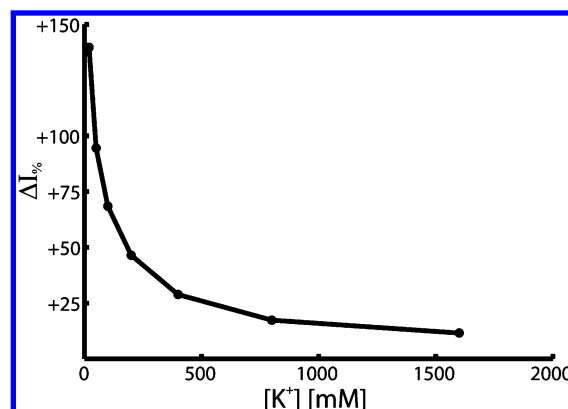


Figure 6. Current increase in the A108E/T112E mutated channel at different bulk concentrations of K^+ . Data on the MthK-based model with the A108E/T112E mutations are shown. The percentage variation in channel current ($\Delta I\%$) refers to the wild-type MthK-based model at the same ion concentration. Membrane potential is set to 100 mV.

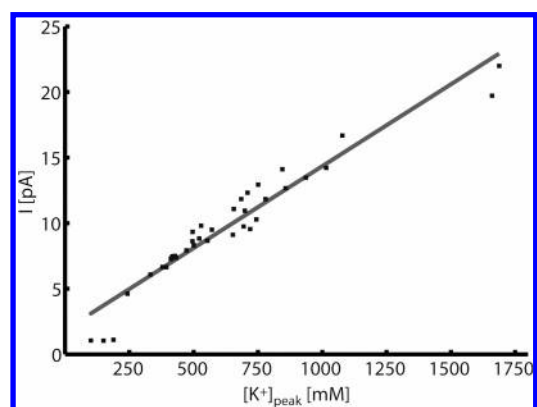


Figure 7. Correlation between Potassium concentration in cavity and channel current. Data of different channel models, charge neutralization schemes, amino acid mutations, and membrane potentials are shown. A square sign is used for the computed currents, a continuous line for the interpolating line.

tuned to account for the confinement effects that must be present in the potassium channels,³⁹ PNP theory reproduces quantitatively the ionic currents and explains the high probability to observe the presence of a K^+ ion below the selectivity filter (intracellular side) in the static picture offered by X-ray crystallography.³⁰ The variability of the channel conductance with amino acid mutations and the role of the protein in the wider region outside the selectivity filter belong by right to the area of applicability of continuum electrodiffusion theory, because this is the region where confinement effects are less marked. In this context, the use of simplified theories, as other recently reported cases of investigation of selectivity^{40,41} or in the study of diffusion through membranes,⁴² allows one to remove unwanted details and highlights the basic principle governing the channel functioning.

The major issues addressed in this work are the functional activity of the P-loop backbone of the proteins, the similar functional activity of the local charges in the M1 and M2 helices, and that of mutated negatively charged residues in the inner helices. The role of the charges of all these moieties is ultimately to modify the potassium ions concentration in the intracellular cavity and, by this, the channel conductance. Channel conductance and potassium concentration are instead not affected by changes in the cavity size, once the intracellular gate is wider than in the KvAP experimental structure. In the PNP theory, electrostatic interactions are the only driving forces acting on ions. Thus, the present analysis shows that the details and the variation of the mechanism of potassium transport are governed by electrostatic interactions.

A correlation between potassium concentration in the intracellular cavity and channel conductance emerged as a propriety of the KcsA channel. Potassium concentration and electric potential in the channel cavity control the driving forces acting on the ions in the selectivity filter. The intracellular vestibule may modulate these driving forces and consequently the channel conductance. Despite that all of the numerical simulations refer to the KcsA channel, we are prone to suggest the concentration–conductance correlation as a general propriety of potassium channels. The hypothesis is supported by the structural conservation of the selectivity filter in the potassium channel family. Structural changes in the intracellular vestibule, like single residue mutations, are not likely to affect the selectivity filter. The filter may be regarded as a functional unit conserved among different potassium channels. In this context, the intracellular vestibule, like other channel moieties, defines the boundaries conditions perceived by the selectivity filter, that is, the ion concentrations and the electric potential, and consequently the channel conductance. Since the selectivity filter is conserved in different potassium channels, the concentration–conductance correlation revealed in KcsA may be valid as a general mechanism. The intracellular cavity couples the selectivity filter to the intracellular compartment, and it may play a pivotal role on the conductivity of potassium channels.

References and Notes

- (1) Hille, B. *Ionic channels of excitable membranes*; Sinauer Associates: Sunderland, MA, 2001.
- (2) Ashcroft, F. M. *Ion channels and disease: channelopathies*; Academic Press: New York, 1999.
- (3) Long, S. B.; Campbell, E. B.; MacKinnon, R. Crystal Structure of a Mammalian Voltage-Dependent Shaker Family K⁺ Channel. *Science* **2005**, 309(5736), 897–903.
- (4) Doyle, D. A.; Cabral, J.; Pfuetzner, R. A.; Kuo, A.; Gulbis, J. M.; Cohen, S. L.; Chait, B. T.; MacKinnon, R. The Structure of the Potassium Channel: Molecular Basis of K⁺ Conduction and Selectivity. *Science* **1998**, 280(5360), 69–77.
- (5) Jiang, Y.; Lee, A.; Chen, J.; Cadene, M.; Chait, B. T.; MacKinnon, R. Crystal structure and mechanism of a calcium-gated potassium channel. *Nature* **2002**, 417(6888), 515–522.
- (6) Jiang, Y.; Lee, A.; Chen, J.; Ruta, V.; Cadene, M.; Chait, B. T.; MacKinnon, R. X-ray structure of a voltage-dependent K⁺ channel. *Nature* **2003**, 423(6935), 33–41.
- (7) Kuo, A.; Gulbis, J. M.; Antcliff, J. F.; Rahman, T.; Lowe, E. D.; Zimmer, J.; Cuthbertson, J.; Ashcroft, F. M.; Ezaki, T.; Doyle, D. A. Crystal Structure of the Potassium Channel KirBac1.1 in the Closed State. *Science* **2003**, 300(5627), 1922–1926.
- (8) Latorre, R.; Oberhauser, A.; Labarca, P.; Alvarez, O. Varieties of Calcium-Activated Potassium Channels. *Ann. Rev. Physiol.* **1989**, 51(1), 385–399.
- (9) Shealy, R. T.; Murphy, A. D.; Ramarathnam, R.; Jakobsson, E.; Subramaniam, S. Sequence-Function Analysis of the K⁺-Selective Family of Ion Channels Using a Comprehensive Alignment and the KcsA Channel Structure. *Biophys. J.* **2003**, 84(5), 2929–2942.
- (10) Grabe, M.; Bichet, D.; Qian, X.; Jan, Y. N.; Jan, L. Y. K⁺ channel selectivity depends on kinetic as well as thermodynamic factors. *Proc. Natl. Acad. Sci.* **2006**, 103(39), 14361–14366.
- (11) Perozo, E.; Marien, D.; Cortes Cuello, L. G. Structural Rearrangements Underlying K⁺-Channel Activation Gating. *Science* **1999**, 285(5424), 73–78.
- (12) Jiang, Y.; Lee, A.; Chen, J.; Cadene, M.; Chait, B. T.; MacKinnon, R. The open pore conformation of potassium channels. *Nature* **2002**, 417(6888), 523–526.
- (13) Jogini, V.; Roux, B. Electrostatics of the Intracellular Vestibule of K⁺ Channels. *J. Mol. Biol.* **2005**, 354(2), 272–288.
- (14) Brelidze, T. I.; Magleby, K. L. Probing the Geometry of the Inner Vestibule of BK Channels with Sugars. *J. Gen. Physiol.* **2005**, 126(2), 105–121.
- (15) Roux, B.; MacKinnon, R. The cavity and pore helices in the KcsA K⁺ channel: stabilization of monovalent cations. *Science* **1999**, 285(5424), 59–61.
- (16) Xu, L.; Wang, Y.; Gillespie, D.; Meissner, G. Two Rings of Negative Charges in the Cytosolic Vestibule of Type-1 Ryanodine Receptor Modulate Ion Fluxes. *Biophys. J.* **2006**, 90(2), 443–453.
- (17) Chen, M. F.; Chen, T. Y. Side-chain Charge Effects and Conductance Determinants in the Pore of CIC-0 Chloride Channels. *J. Gen. Physiol.* **2003**, 122(2), 133–145.
- (18) Fujiwara, Y.; Kubo, Y. Functional Roles of Charged Amino Acid Residues on the Wall of the Cytoplasmic Pore of Kir2.1. *J. Gen. Physiol.* **2006**, 127(4), 401–419.
- (19) Li, R. A.; Velez, P.; Chiamvimonvat, N.; Tomaselli, G. F.; Marban, E. Charged Residues between the Selectivity Filter and S6 Segments Contribute to the Permeation Phenotype of the Sodium Channel. *J. Gen. Physiol.* **1999**, 115(1), 81–92.
- (20) Smith, S. S.; Liu, X.; Zhang, Z. R.; Sun, F.; Kriewall, T. E.; McCarty, N. A.; Dawson, D. C. CFTR: Covalent and Noncovalent Modification Suggests a Role for Fixed Charges in Anion Conduction. *J. Gen. Physiol.* **2001**, 118(4), 407–432.
- (21) Imoto, K.; Busch, C.; Sakmann, B.; Mishina, M.; Konno, T.; Nakai, J.; Bujo, H.; Mori, Y.; Fukuda, K.; Numa, S. Rings of negatively charged amino acids determine the acetylcholine receptor channel conductance. *Nature* **1988**, 335(6191), 645–648.
- (22) Nimigeon, C. M.; Chappie, J. S.; Miller, C. Electrostatic Tuning of Ion Conductance in Potassium Channels. *Biochemistry* **2003**, 42(31), 9263–9268.
- (23) Brelidze, T. I.; Niu, X.; Magleby, K. L. A ring of eight conserved negatively charged amino acids doubles the conductance of BK channels and prevents inward rectification. *Proc. Natl. Acad. Sci.* **2003**, 100(15), 9017–9022.
- (24) Zhou, Y.; Morais-Cabral, J. H.; Kaufman, A.; MacKinnon, R. Chemistry of ion coordination and hydration revealed by a K⁺ channel-Fab complex at 2.0 Å resolution. *Nature* **2001**, 414(6859), 43–48.
- (25) Case, D. A.; Darden, T. A.; Cheatham, T. E.; Simmerling, C. L.; Wang, J.; Duke, R. E.; Luo, R.; Merz, K. M.; Wang, B.; Pearlman, D. A.; Crowley, M.; Brozell, S.; Tsui, V.; Gohlke, H.; Mongan, J.; Hornak, V.; Cui, G.; Beroza, P.; Shafmeister, C.; Calwell, J. W.; Ross, W. S.; Kolmann, P. A. *AMBER 8*; University of California: San Francisco, 2004.
- (26) Berneche, S.; Roux, B. The Ionization State and the Conformation of Glu-71 in the KcsA K⁺ Channel. *Biophys. J.* **2002**, 82(2), 772–780.
- (27) Notredame, C.; Higgins, D.; Heringa, J. T-Coffee: A novel method for multiple sequence alignments. *J. Mol. Biol.* **2000**, 302, 205–217.
- (28) Volkov, A. G.; Paula, S.; Deamer, D. W. Two mechanisms of permeation of small neutral molecules and hydrated ions across phospholipid bilayers. *Bioelectrochem. Bioenerg.* **1997**, 42, 153–160.
- (29) Guex, N.; Peitsch, M. C. SWISS-MODEL and the Swiss-Pdb-Viewer: An environment for comparative protein modeling. *Electrophoresis* **1997**, 18, 2714–2723.
- (30) Furini, S.; Zerbetto, F.; Cavalcanti, S. Application of the Poisson-Nernst-Planck Theory with Space-Dependent Diffusion Coefficients to KcsA. *Biophys. J.* **2006**, 91(9), 3162–3169.
- (31) Lide, D. R. *CRC handbook of chemistry and physics*; CRC Press: Boca Raton, FL, 2004.
- (32) Allen, T. W.; Kuyucak, S.; Chung, S. H. Molecular dynamics estimates of ion diffusion in model hydrophobic and KcsA potassium channels. *Biophys. Chem.* **2000**, 86(1), 1–14.
- (33) Mamonov, A. B.; Kurnikova, M. G.; Coalson, R. D. Diffusion constant of K⁺ inside Gramicidin A: A comparative study of four computational methods. *Biophys. Chem.* **2006**, 124(3), 268–278.
- (34) Nina, M.; Beglov, D.; Roux, B. Atomic Radii for Continuum Electrostatics Calculations Based on Molecular Dynamics Free Energy Simulations. *J. Phys. Chem. B* **1997**, 101(26), 5239–5248.
- (35) LeMasurier, M.; Heginbotham, L.; Miller, C. KcsA: It's a Potassium Channel. *J. Gen. Physiol.* **2001**, 118(3), 303–314.
- (36) Garofoli, S.; Jordan, P. C. Modeling Permeation Energetics in the KcsA Potassium Channel. *Biophys. J.* **2003**, 84(5), 2814–2830.
- (37) Chatelain, F. C.; Alafem, N.; Xu, Q.; Pancaroglu, R.; Reuveny, E.; Minor, J. The Pore Helix Dipole Has a Minor Role in Inward Rectifier Channel Function. *Neuron* **2005**, 47(6), 833–843.
- (38) Nonner, W.; Chen, D. P.; Eisenberg, B. Progress and Prospects in Permeation. *J. Gen. Physiol.* **1999**, 113(6), 773–782.

(39) Corry, B.; Kuyucak, S.; Chung, S. H. Tests of Continuum Theories as Models of Ion Channels. II. Poisson-Nernst-Planck Theory versus Brownian Dynamics. *Biophys. J.* **2000**, 78(5), 2364–2381.

(40) Bostick, D. L.; Brooks, C. L., III Selectivity in K⁺ channels is due to topological control of the permeant ion's coordinated state. *Proc. Natl. Acad. Sci.* **2007**, 104(22), 9260–9265.

(41) Boda, D.; Nonner, W.; Valisko, M.; Henderson, D.; Eisenberg, B.; Gillespie, D. Steric Selectivity in Na Channels Arising from Protein Polarization and Mobile Side Chains. *Biophys. J.* **2007**, 93, 1960–1980.

(42) Shaw, R. S.; Packard, N.; Schroter, M.; Swinney, H. L. Geometry-induced asymmetric diffusion. *Proc. Natl. Acad. Sci.* **2007**, 104(23), 9580–9584.